Creep Microstructural Evolution of Type IV Cracking in Long-Serviced Dissimilar Steel Welded Joints

Zihao Shen [a], Fei Gao [b], Denghui Wang [c], Yuan Li [d], Zheng Zhang *

School of Materials Science and Engineering, Beihang University, Beijing 100191, China

* Corresponding author: Zheng Zhang (Email: zhangzh@buaa.edu.cn), [a] 13583617829@163.com,

[b] gaofei520@buaa.edu.cn, [c] wangdh@buaa.edu.cn, [d] 18811327152@163.com

Abstract. A high-temperature creep interruption test at 650°C and 70 MPa was conducted on a long-serviced T92-Super304H welded joint to study Type IV cracking and service-induced damage. The fine-grained heat-affected zone (FGHAZ) displayed lath degradation, precipitate coarsening, and grain boundary damage. During creep, recrystallization and grain recovery occurred in the FGHAZ on the T92 side. Dislocations aggregated around precipitates and at damaged grain boundaries, where Type IV cracks formed and propagated. This accumulation and boundary damage are main mechanisms of Type IV cracking.

Keywords: Long-serviced Dissimilar Steel Welded; Heat Affected Zone; Type IV Crack; Grain Boundary Damage.

1. Introduction

In ultra-supercritical power units, the application of dissimilar steel welded pipes is widespread, providing both functional capability for steam transportation and cost-efficient performance improvements[1]. Pipelines using T92 martensitic steel and Super304H austenitic steel as welding materials are quite common[2]. During the welding process, both metals undergo microstructural changes in the heat-affected zone (HAZ) due to the applied welding heat[3]. On the T92 steel side, the HAZ extends from the weld nugget to the base metal (BM) and is divided into coarse-grained heat-affected zone (CGHAZ), fine-grained heat-affected zone (FGHAZ), and intermediate critical heat-affected zone (ICHAZ). In contrast, the grain size on the Super304H steel side progressively decreases from the weld nugget toward the base metal[2]. The HAZ significantly alters the mechanical properties of the welded joint, presenting safety concerns in engineering applications. While failures are rare on the austenitic steel side, Type IV cracks frequently develop on the martensitic T92 side during high-temperature creep, leading to economic losses in power plants[4].

Type IV cracking primarily results from the vulnerability of the fine-grained heat-affected zone of T92 steel under high-temperature creep conditions, causing brittle fractures[5]. Damage is concentrated in T92, with failure locations shifting from the base material to the FGHAZ as creep duration increases[6]. The mechanical strength of the HAZ diminishes more rapidly than that of the base material, due to accelerated tempering and preferential precipitation of the Laves phase at grain boundaries[3], which contributes to premature failure[7].

In practical power plant operations, safety risks escalate with service time as the martensitic steel experiences internal damage under ultra-supercritical conditions. Although T92 steel possesses excellent mechanical properties, long-term service leads to microstructural changes, including Laves phase formation, coarsening of precipitates, and recovery of the tempered martensite matrix, significantly reducing creep resistance[8]. The creep fracture behavior of unserved welded joints under high stress differs from low-stress, long-serviced joints. Existing research mainly focuses on non-service high-stress conditions, where BM failures are common, and lacking Type IV cracking in low-stress pipelines operated for tens of thousands of hours. This study aims to explore the microstructural evolution of Type IV cracking in dissimilar steel welded joints after 80,000 hours of low-stress service.

2. Experimental Section

The experimental material is a T92-Super304H steel welded joint that has been in service for 80,000 hours, and the morphology is shown in Figure 1(a). A 100 mm specimen was used for the high-temperature creep experiment, with the specimen dimensions illustrated in Figure 1(b).



Figure 1. (a)Welded joint of dissimilar steels used in the experiment; (b)Dimensions of high-temperature creep specimens

The high-temperature creep interruption test was designed based on the duration of high-temperature creep fracture (t_m), with interruption times set at 20%t_m, 50%t_m, and 80%t_m. The experimental condition was 650°C, 70 MPa. A corrosion solution was prepared using ferric chloride (10 g), hydrochloric acid (40 ml), and water (40 ml) to corrode the specimen. The microstructure of the post-creep specimen cross-section was observed using scanning electron microscopy (SEM), electron backscatter diffraction (EBSD), and transmission electron microscopy (TEM).The model of the scanning electron microscope (SEM) used was JSM-6010, the EBSD model was JSM-7900F, and the transmission electron microscope (TEM) model was JEM-2010.

3. Results

3.1 Microstructure of Dissimilar Steel Welded Joint

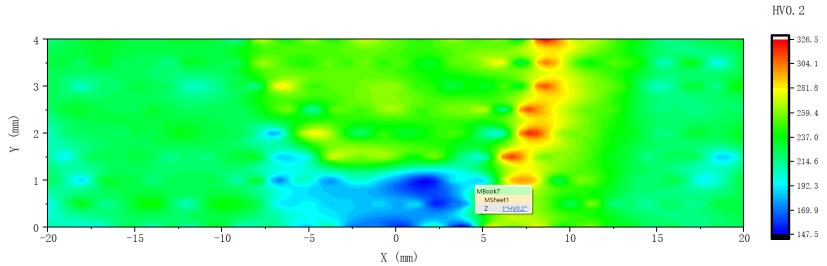


Figure 2. Microhardness distribution map of dissimilar steel welded joints

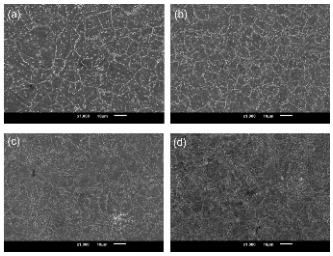


Figure 3. Microstructural features: (a) CGHAZ; (b) FGHAZ; (c) ICHAZ; (d) BM

The microhardness of a long-serviced dissimilar steel welded joint was tested and the experimental results shown in Figure 2. On the T92 side, the highest hardness value was 322 HV in the coarse-grained heat-affected zone (HAZ), but the hardness values in the FGHAZ and ICHAZ, where cracks form, decreased rapidly, creating a distinct hardness gradient. On the Super304H side, the lowest hardness value was 150 HV.

The surface morphology on the T92 side where cracks form is shown in Figure 3. In Figure 3(a), the CGHAZ shows the uniform precipitation with very clear grain boundaries. In Figure 3(b), the FGHAZ has smaller grains and less dense precipitates, relatively clear grain structures, and less

distinct grain boundaries. Figure 3(c) shows significantly reduced grain boundary clarity and further reduced precipitation phase density of ICHAZ compared to the FGHAZ. In Figure 3(d), the BM area has blurred grain boundaries, and the most dispersed precipitation phase, exhibiting clear characteristics of long-term service damage.

3.2 High-temperature Creep Performance of Dissimilar Steel Welded Joints

The high-temperature creep test results for the dissimilar steel welded joint are presented in Table 1, with a creep fracture time of 822 hours. Under the experimental conditions of 650°C and 70 MPa, the creep specimen fractured in the FGHAZ, as shown in Figure 4(a). Figure 4(b) illustrates the fracture surface morphology, which exhibits brittle intergranular fracture with precipitate particles on the fracture surface. The fracture location in the creep specimen is a typical region for Type IV cracking.

Table 1. High-temperature creep test results for dissimilar steel welded joints

Temperature(°C)	Stress(MPa)	Time(h)	Shrinkage(%)	Elongation(%)
650	70	822	28	4.0

Based on this, high-temperature creep interruption experiments were designed with durations of 161 hours, 411 hours, and 658 hours. The results of creep interruption tests are presented in Table 2.

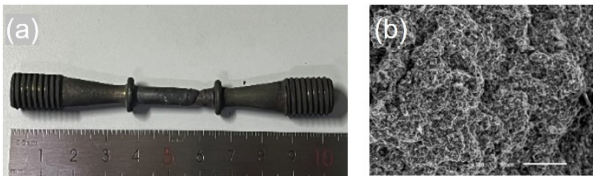


Figure 4. (a) fracture location in high-temperature creep specimens; (b)Fracture morphology of dissimilar steel welded joints

Table 2. Results of interrupted creep experiments on dissimilar steel welded joints

Sample number	Stress (Mpa)	Time (h)	Elongation (%)
8w-70-20%	70	161	2.4
8w-70-50%	70	411	3.5
8w-70-80%	70	658	3.9

3.3 Microstructural Evolution During Creep of Dissimilar Steel Welded Joints

Microhardness tests were conducted on the creep interruption specimens with results shown in Figure 5. At an interruption time of 20% creep life, or 161 hours, the specimen's microhardness value is displayed in Figure 5(a), showing little reduction and the highest hardness in the coarse-grained area on the T92 side. As creep time increases to 411 hours, as shown in Figure 5(b), there is a significant drop in microhardness on the T92 side, along with a rapid decrease in the hardness of the weld nugget structure near the T92 side. In Figure 5(c), when the creep time reaches 658 hours, which is 80% of the creep life, the lowest microhardness value on the T92 side is 35 HV. The variation in microhardness on the Super304H side is less pronounced.

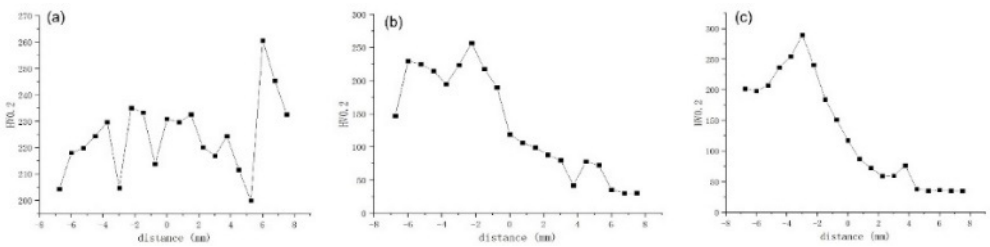


Figure 5. Hardness of interrupted specimens: (a) 161h; (b) 411h; (c) 822h

The grain size in the FGHAZ of the creep interruption specimen is illustrated in Figure 6. With increasing creep time, the proportion of small-sized grains gradually decreases, with most becoming medium-sized grains. As shown in Figure 6(d), at 658 hours of creep time, large grains with diameters exceeding 20 μm are also observed.

During the high-temperature creep process, the proportions of different grain types are shown in Figure 7 which is a Grain Orientation Spread (GOS) map. The proportion of recrystallized grains (in blue) initially increases with creep time and later decreases, while the proportions of recovered and deformed grains gradually increase after 411 hours of creep time. In Figure 7(d), a noticeable increase in grain size is observed, with many recrystallized grains transforming into recovered grains, and the number of deformed grains increasing compared to earlier samples.

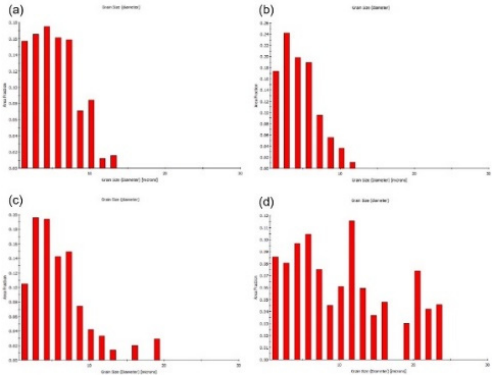


Figure 6. Grain size of interrupted specimens: (a) 0h; (b) 161h; (c) 411h; (d) 822h

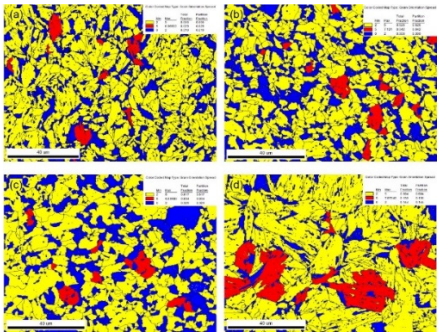


Figure 7. GOS maps of interrupted specimens: (a) 0h; (b) 161h; (c) 411h; (d) 822h

After the creep interruption reached 80% of creep life, or 658 hours, TEM observations of the fine-grained heat-affected zone on the T92 side, shown in Figure 8(a), revealed significant dislocation accumulation around precipitates and at grain boundaries. In Figure 8(b), precipitates are also observed aggregating at the edges of grain boundaries. Numerous creep voids appeared near the high-temperature creep fracture surface, all located in the fine-grained heat-affected zone shown in Figure 8(c).

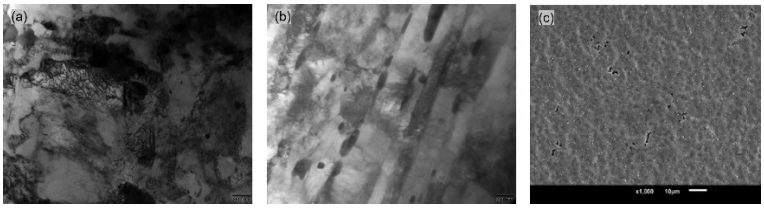


Figure 8. TEM images of 8w-70-80%: (a) Dislocation; (b) Precipitate phase; (c) Cross-sectional view of the FAHAZ Creep voids

4. Discussion

Microhardness tests and microscopic analysis of long-serviced dissimilar steel welded joints reveal significant structural changes. Initially, during welding on the T92 side, the CGHAZ reaches the highest temperatures, fully melting and uniformly re-precipitating phases upon cooling, resulting in the highest microhardness. In contrast, the FGHAZ experiences lower temperatures that partially melt precipitates, leading to uneven distribution and smaller grains, thereby reducing microhardness. ICHAZ is chiefly affected by heat treatment temperatures.

After 80,000 hours of service, the FGHAZ, ICHAZ, BM on the T92 side show blurred grain boundaries, lath degradation, and coarsening of precipitate phases relative to the coarse-grained zone, further decreasing microhardness. These changes in the fine-grained and critical zones contribute to a gradient in microhardness and grain boundary structures, fostering Type IV crack initiation.

High-temperature creep tests indicate that under 650°C and 70 MPa, brittle fractures occur in the fine-grained HAZ after 822 hours. Under these conditions, dissimilar steel welded joints are vulnerable to Type IV cracks, especially in the T92 FGHAZ, where microhardness gradients are most pronounced. Creep interruption experiments show that during early creep stages, grain sizes in the T92 FGHAZ are small. However, prolonged stress leads to grain growth, externally influencing Type IV fracture initiation. Internal grains within this zone deform, transitioning to deformed grains and weakening the welded joint's integrity.

In the later creep stages, dislocation and precipitate accumulation intensify around grain boundaries, promoting Type IV cracks. Thus, grain boundary damage from 80,000 hours of service exacerbates susceptibility to cracking during high-temperature creep, allowing cracks to originate and propagate, resulting in Type IV failure.

5. Conclusion

This paper investigates the evolution of creep microstructure of Type IV cracking in dissimilar steel welded joints after long service. The conclusions are as follows:

1. After 80,000 hours of service, the microstructure of T92 steel significantly degraded, exhibiting martensitic lath degeneration, grain boundary damage, and coarsening of precipitate phases.

2. Under creep test conditions of 650°C and 70 MPa, brittle intergranular Type IV cracking occurred in the FGHAZ of T92, indicating its susceptibility to high-temperature creep failure.

3. Type IV cracking results from long-term service conditions that damage grain boundaries and coarsen precipitate phases, coupled with recrystallization during creep. These processes lead to dislocation and precipitate accumulation at damaged boundaries, initiating and propagating cracks, ultimately causing brittle fractures.

Acknowledgments

This work is supported by the National key Research and Development Program (2021YFC3001 801-03).

References

[1] G. Dak, C. Pandey, A critical review on dissimilar welds joint between martensitic and austenitic steel for power plant application, Journal of Manufacturing Processes 58 (2020) 377-406.

[2] Z. Liang, Y. Gui, Q. Zhao, Investigation of Microstructures and Mechanical Properties of T92 Martensitic Steel/Super304 Austenitic Steel Weld Joints Made with Three Welding Consumables, Archives of Metallurgy and Materials (2018) 1249-1256.

[3] J. Deng, Z. Liang, S.e. Hui, Q. Zhao, Aging Treatment on the Microstructures and Mechanical Properties of New Groove T92/Super 304H Dissimilar Steel Joints, High Temperature Materials and Processes 34(5) (2015).

[4] M.-Y. Kim, S.-C. Kwak, I.-S. Choi, Y.-K. Lee, J.-Y. Suh, E. Fleury, W.-S. Jung, T.-H. Son, High-temperature tensile and creep deformation of cross-weld specimens of weld joint between T92 martensitic and Super304H austenitic steels, Materials Characterization 97 (2014) 161-168.

[5] H. Tsuruta, H. Toda, K. Hirayama, K. Shimizu, H. Fujihara, A. Takeuchi, M. Uesugi, The spatial and temporal characterization of type IV creep fracture in notched specimen of modified 9Cr-1Mo steel, Materials Science and Engineering a-Structural Materials Properties Microstructure and Processing 902 (2024).

[6] M. Nie, J. Zhang, F. Huang, J.W. Liu, X.K. Zhu, Z.L. Chen, L.Z. Ouyang, Microstructure evolution and life assessment of T92 steel during long-term creep, Journal of Alloys and Compounds 588 (2014) 348-356.

[7] J. Cao, Y. Gong, Z.-G. Yang, Microstructural analysis on creep properties of dissimilar materials joints between T92 martensitic and HR3C austenitic steels, Materials Science and Engineering: A 528(19-20) (2011) 6103-6111.

[8] K. Sawada, K. Suzuki, H. Kushima, M. Tabuchi, K. Kimura, Effect of tempering temperature on Z-phase formation and creep strength in 9Cr–1Mo–V–Nb–N steel, Materials Science and Engineering: A 480(1-2) (2008) 558-563.